

Article

The Synthesis, Crystal Structure, and Magnetic Properties of Mono-Scorpionate Eu(III) Complexes

Kira E. Vostrikova , Taisiya S. Sukhikh  and Alexander N. Lavrov

Nikolayev Institute of Inorganic Chemistry, Siberian Branch of Russian Academy of Sciences, 630090 Novosibirsk, Russia; sukhikh@niic.nsc.ru (T.S.S.); lavrov@niic.nsc.ru (A.N.L.)

* Correspondence: vosk@niic.nsc.ru

Abstract: Three Eu^{3+} complexes containing a neutral tripodal ligand possessing a predictable coordination mode have been obtained and studied. The trispyrazolylmethane complexes have an aqua ligand in the coordination sphere, forming both the mononuclear species $[\text{Eu}(\text{HCPz}_3)\text{H}_2\text{O}(\text{NO}_3)_3]$ and the dimer $[\text{Eu}(\text{HCPz}_3)\text{H}_2\text{O}(\text{CF}_3\text{SO}_3)_3]_2$, having a *Chinese lantern* structure, whereas the use of the methylated tripod leads to the water-free complex, $[\text{Eu}(\text{HC}(\text{Pz}^{\text{Me}}_2)_3)(\text{NO}_3)_3]$. A qualitative analysis of the magnetic susceptibility of polycrystalline samples demonstrated that the magnetic properties can be described using a simple Van Vleck formula with spin–orbit coupling parameter ($\lambda = 383 \div 406 \text{ cm}^{-1}$) close to the values for free Eu^{3+} ions. The stereochemical analysis of the coordination environment of $[\text{Ln}(\text{HC}(\text{Pz}^{\text{Me}}_2)_3)(\text{NO}_3)_3]$ has shown that these complexes can be used as diamagnetic model systems to obtain information on the crystal field effects in the paramagnetic monoradical complexes, $[\text{LnRad}(\text{NO}_3)_3]$, since both types of compounds have the same type of coordination polyhedron (symmetry point group D_{3h}) and very close Ln–donor atom distances.

Keywords: europium(III) complexes; scorpionate; tripodal ligand; trispyrazolylmethane; tris(3,5-dimethyl-1-pyrazolyl)methane; magnetic properties; spin–orbit coupling



Citation: Vostrikova, K.E.; Sukhikh, T.S.; Lavrov, A.N. The Synthesis, Crystal Structure, and Magnetic Properties of Mono-Scorpionate Eu(III) Complexes. *Inorganics* **2023**, *11*, 418. <https://doi.org/10.3390/inorganics11100418>

Academic Editors: Leonor Maria and Joaquim Marçalo

Received: 23 August 2023

Revised: 13 October 2023

Accepted: 18 October 2023

Published: 23 October 2023



Copyright: © 2023 by the authors. Licensee MDPI, Basel, Switzerland. This article is an open access article distributed under the terms and conditions of the Creative Commons Attribution (CC BY) license (<https://creativecommons.org/licenses/by/4.0/>).

1. Introduction

The design of molecular materials with newly developed functionalities holds the potential for technological advances. Materials based on molecules that switch under the action of various stimuli will form the basis for the creation of multifunctional devices that combine optical, magnetic, and other electronic properties, as well as extreme miniaturization. For these purposes, understanding what the fundamental properties of molecular coordination compounds depend on, and how they can be controlled, is very important for the creation of new functional molecular materials.

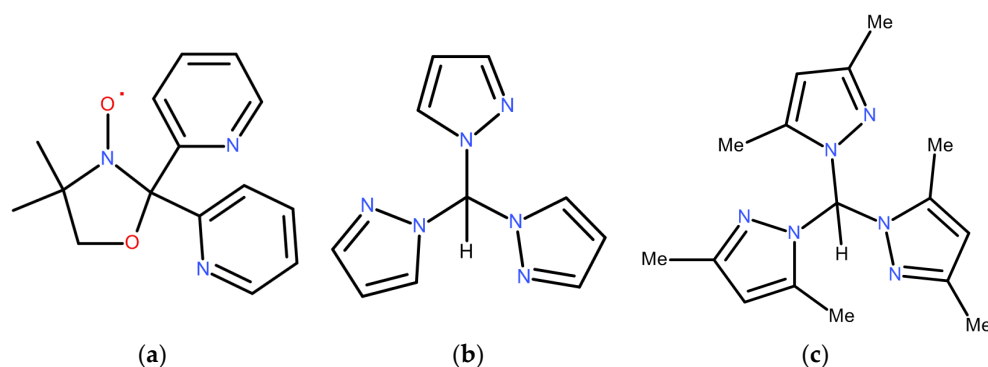
The unique electronic and physical properties of rare-earth ions are used for various applications, including the development of magnetic and luminescent materials. In this direction, the main attention is paid to the design of luminescent single-molecule magnets (SMMs), which requires the development of rational approaches to the search for compounds with strong magnetic anisotropy and enhanced photoluminescence [1,2].

The main candidates for the role of SMMs are lanthanide (Ln) complexes, in which the metal ion is in the trivalent state and the redox activity is usually limited to the ligand. However, lanthanide-based redox activity is also possible. Among the lanthanides, europium possesses the most reachable divalent oxidation state, Eu^{2+} , because of its half-filled $4f^7$ electronic configuration [3,4]. For this reason, a vast majority of the magnetically studied Eu^{3+} molecular complexes contain some amount of Eu^{2+} ($S = 7/2$) impurities, which can be easily detected through low-temperature magnetic susceptibility measurements [5,6]. To date, there is abundant information on the photophysical properties of Eu^{3+} molecular complexes, which are quite well studied spectroscopically. At the same time, because the ground-state multiplet 7F_0 of Eu^{3+} ions is non-magnetic ($S = L = 3$; $J = S - L = 0$),

researchers often leave the magnetic properties of europium luminescent compounds unattended. However, owing to the excited multiplets that are located closely in energy to the ground-state one, Eu^{3+} ions exhibit a considerable magnetic activity associated with Van Vleck paramagnetism at low temperatures and the thermal population of the excited states that is already manifested at moderate temperatures, with the effective magnetic moment reaching a value of $\sim 3.2 \mu_B$ at room temperature. In its turn, the low redox potential of the $\text{Eu}^{2+}/\text{Eu}^{3+}$ pair [7] in combination with non-innocent organic ligands can lead to interesting materials both photo- and magnetically switchable, including SMMs [8,9].

Tuning the electronic properties of a compound is the most common challenge for materials scientists. This can be achieved by varying the ligand environment of a central atom, namely the polyhedron geometry and the ligand field strength. The latter is mainly determined by nature of the donor atoms, whereas the former depends not only on the ligand geometry but also on its coordination manner. Organic tripod molecules with donor atoms on each of the three legs are most promising for the chemical construction of various complexes with a predictable geometry. Moreover, the latter can be easily adjusted using methods of synthetic organic chemistry.

Previously, we have obtained the monoradical $[\text{LnRad}(\text{NO}_3)_3]$ ($\text{Ln}^{3+} = \text{Gd}, \text{Tb}, \text{Dy}, \text{Tm}$ [10] and biradical $[\text{Ln}(\text{Rad})_2(\text{OTf})_3]$ ($\text{Ln}^{3+} = \text{Eu}$ and Dy) [11] complexes, where Rad is a tripodal nitroxyl radical (Scheme 1a), 4,4-dimethyl-2,2-bis(pyridin-2-yl)-1,3-oxazolidine-3-oxyl. Upon comparing the magnetic susceptibility ($\chi_M T$) measured for the biradical Eu complex (1.78 and 0.348 emuK/mol at 300 and 2 K, respectively) [11] with the values known for the $[\text{Eu}(\text{radical})_2(\text{anion})_3]$ compounds [12–18], we noticed a remarkable dispersion of $\chi_M T$ in the latter, varying from 1.89 to 3.09 emuK/mol at room temperature, and from 0.035 to 0.42 emuK/mol at low temperatures. Correspondingly, the theoretical estimates of the magnetic parameters for Eu^{3+} biradical complexes that are reported in the literature resulted in a surprisingly large scatter in the values of the spin–orbit coupling (SOC) parameter, λ . In turn, in the case of monoradical $[\text{Eu}(\text{radical})(\text{anion})_3]$ complexes, there is no reasonable explanation for the deviation of their magnetic susceptibility, measured at low temperatures ($\chi_M T = 0.192\text{--}0.252$ emuK/mol) [19–21], from the value of 0.375 emuK/mol, naturally expected for radicals with $S = 1/2$ non-interacting with the Eu^{3+} ion's singlet state. The observed discrepancies point to an insufficient understanding of the interaction between the Eu^{3+} ions with strong SOC and paramagnetic ligands.



Scheme 1. The tripodal ligands: (a) 4,4-dimethyl-2,2-bis(pyridin-2-yl)-1,3-oxazolidine-3-oxyl (Rad); (b) Trispyrazolylmethane (HCPz_3); (c) tris(3,5-dimethyl-1-pyrazolyl)methane ($\text{HC}(\text{Pz}^{\text{Me}}_2)_3$).

In order to clarify the nature of Eu^{3+} –Rad interaction one can compare, for example, the complexes with paramagnetic and diamagnetic ligands, $[\text{EuRad}(\text{NO}_3)_3]$ and $[\text{EuL}_{\text{dia}}(\text{NO}_3)_3]$. The latter is a model complex containing a diamagnetic tripodal ligand with a coordination polyhedron geometry that is close to that of the radical complex. Such a strategy of diamagnetic substitution was used for obtaining information on the crystal field (CF) effects in paramagnetic Ln ions [15,22,23]. For instance, for two homologous series of coordination compounds, $[\text{LnNN}^{\text{trz}}_2(\text{NO}_3)_3]$ and $[\text{Ln}(\text{Nitron})_2(\text{NO}_3)_3]$ [15], and $[\text{Ln}(\text{HBPz}_3)_2\text{SQ}]$ and $[\text{Ln}(\text{HBPz}_3)_2\text{Trp}]$ [22,23], where NN^{trz} is 2-(4',5'-dimethyl-1',2',3'-

triazolyl)-4,4,5,5-tetramethyl-4,5-dihydro-1H-imidazolyl-1-oxy-3-oxide, and SQ is 3,5-di-tert-butylsemiquinonato, respectively, while the diamagnetic homologue ligands, Nitron and Trp, are 3-N-tert-butylnitron-4,5-dimethyltriazole and tropolonate, correspondingly. In the present case of Eu complexes, this experimental approach should help to elucidate the nature of coupling between the radical and Eu^{3+} ion by subtracting the CF splitting effect.

In this paper, we have synthesized and magnetically studied three Eu^{3+} complexes comprising diamagnetic tripodal pyrazolyl-based ligands (see Scheme 1b,c) to determine the reference values of the magnetic susceptibility for such Eu(III) complexes, and to establish a ground for further studies of the Eu^{3+} -Rad interactions in complexes with a similar geometry of the coordination polyhedron.

2. Short Theoretical Background

Trivalent europium ions (Eu^{3+}) exhibit intense red photoluminescence upon irradiation with ultra violet light [24]. This luminescence is observed not only for Eu^{3+} ions doped into crystalline host matrices or glasses, but also for europium(III) complexes with organic ligands [25]. Such a ligand can drastically enhance the photoluminescence quantum yield by acting as an “antenna” to absorb the excitation light and to transfer the energy to the Eu^{3+} ion, thereby bringing about the population of excited Eu^{3+} energy levels, including the emitting one [2]. Not only its red luminescence, but also the narrow transitions in the luminescence spectra are typical features of the Eu^{3+} ion [26], and these spectroscopic properties have been known since the earliest history of the chemical element europium [27]. Many Eu^{3+} compounds show an intense photoluminescence due to the ${}^5D_0 \rightarrow {}^7F_J$ transitions ($J = 0-6$) from the 5D_0 excited state to the J levels of the ground term 7F . The fine structure and the relative intensities of the transitions in the luminescence spectra of Eu^{3+} can be used to probe the local surroundings of the metal center. Spectroscopic experimental data provide information on the point group symmetry of the Eu^{3+} site, as well as on the polyhedron geometry [26], which is especially useful for solution studies. Other techniques can also be used for the determination of the CF energy levels inside the $4f$ shell, including two-photon absorption, Zeeman spectroscopy, and magnetic circular dichroism [24].

To a first approximation, a lanthanide central atom in a molecular coordination compound behaves as an Ln^{3+} free ion, for which the paramagnetic behavior is due to its unpaired $4f$ electrons. As these electrons are shielded by the outer electronic closed shell ($2p$), the Coulomb electron–electron interaction and spin–orbit coupling between $4f$ electrons are much stronger than the ligand field, and hence, the former plays a decisive role in the electronic level structure and magnetic properties. Depending on the sign of the spin–orbit interaction, the total magnetic moment (J) of a Ln^{3+} ion is formed as $J = L \pm S$, where L is the angular momentum and S is the spin momentum. For the majority of Ln^{3+} ions, the ${}^{2S+1}L_J$ ground-state (GS) multiplet is well-isolated in energy from the first excited one. Then, only the GS is thermally populated in the temperature range of 0–300 K. In the free ion approximation, the molar magnetic susceptibility for a mononuclear species is given in Equation (1) [28]:

$$\chi_J = \frac{Ng_J^2\beta^2J(J+1)}{3kT} + \frac{2N\beta^2(g_J-1)}{3\lambda} \quad (1)$$

where λ is the spin–orbit coupling parameter and g_J is equal to

$$g_J = \frac{3}{2} + \frac{[S(S+1) - L(L+1)]}{2J(J+1)} \quad (2)$$

For $J = 0$, there is obviously no first-order Zeeman splitting. However, the application of a magnetic field can result in second-order splitting and the appearance of a net magnetic moment. The last part in (1) is a temperature-independent contribution arising from the coupling between the ground and excited states. For Ln molecular compounds, the χ_{MT} versus T curve often differs slightly from what is predicted by (1). This deviation occurs for

two reasons: the crystal field partially removing the $2J + 1$ degeneracy of the GS in zero-field, and the thermal population of the Ln^{3+} excited states. The latter is most pronounced for tri-positive Sm and Eu, which possess excited states that are located closely in energy to the ground one. In the case of Eu^{3+} , its 7F ground term is splitted by SOC into seven multiplets (${}^7F_0, {}^7F_1, {}^7F_2, {}^7F_3, {}^7F_4, {}^7F_5, {}^7F_6$) with energies of $E(J) = \lambda J(J + 1)/2$, where the energy of the 7F_0 ground state is taken as zero. Since λ is small enough for the excited states to be thermally populated, the magnetic susceptibility may be written as

$$\chi_M = \frac{\sum_{J=0}^6 (J + 1) \chi_J e^{-\frac{\lambda J(J+1)}{2kT}}}{\sum_{J=0}^6 (2J + 1) \chi_J e^{-\frac{\lambda J(J+1)}{2kT}}} \quad (3)$$

where χ_J is given in Equation (1). In the case of Eu^{3+} , all of the g_J are equal to $3/2$, except g_0 , which is equal to $2 + L(=2 + S) = 5$, i.e., $(\chi_M T)_{\text{Eu}}$ can be expanded as [29]

$$\frac{N\beta^2}{3kx} \left[24 + \left(\frac{27}{2}x - \frac{3}{2}\right)e^{-x} + \left(\frac{135}{2}x - \frac{5}{2}\right)e^{-3x} + (189x - \frac{7}{2})e^{-6x} + (405x - \frac{9}{2})e^{-10x} + \left(\frac{1485}{2}x - \frac{11}{2}\right)e^{-15x} + \left(\frac{2457}{2}x - \frac{13}{2}\right)e^{-21x} \right] \\ \left[1 + 3e^{-x} + 5e^{-3x} + 7e^{-6x} + 9e^{-10x} + 11e^{-15x} + 13e^{-21x} \right] \quad (4)$$

where $x = \lambda/kT$.

At moderate temperatures, owing to the value of $\lambda \sim 350 \text{ cm}^{-1}$ [28], only the first three lower states (${}^7F_0, {}^7F_1, {}^7F_2$), with energies of $0, \lambda$, and 3λ , can be considerably populated; since the 7F_0 ground state is formally nonmagnetic, the lower limit of χT is zero. However, the low-temperature limit of the magnetic susceptibility, χ_{LT} , is non-zero due to the temperature-independent contribution arising from the coupling between the ground and excited states. According to Equation (4), which acquires a very simple form in the $T = 0$ limit, the χ_{LT} value is directly related to λ as

$$\chi_{LT} = 8N\beta^2/\lambda = 2.085/\lambda \quad (\lambda \text{ in } \text{cm}^{-1}) \quad (5)$$

Although the aforementioned description has been proven to capture the main qualitative features of the magnetic susceptibility of europium(III)-based compounds, its performance turns out to be not as good when it comes to the precise determination of λ and quantitative comparison with spectroscopic results. The problem stems from the CF splitting of the excited $J \neq 0$ multiplets, which is not taken into account in Equation (4) [29–31]. Given that the 7F_1 multiplet is the closest one in energy to the ground level, its splitting into three Stark sublevels plays the most important role. For example, when one considers the low-temperature magnetic susceptibility and allows for the splitting of the first excited multiplet, Equation (5) turns into

$$\chi_{LT} = (8N\beta^2/3)(1/E_1 + 1/E_2 + 1/E_3) \quad (6)$$

where E_1, E_2, E_3 are the energies of the 7F_1 multiplet sublevels. Apparently, when the multiplet splitting is negligible, Equations (5) and (6) are equivalent, as $1/E_1 = 1/E_2 = 1/E_3 = 1/\lambda$. But, in the opposite case of strong splitting, the average $(1/E_1 + 1/E_2 + 1/E_3)/3$ becomes significantly larger than $1/\lambda$, resulting in the magnetic susceptibility in the low-temperature plateau region to be enhanced compared to the values predicted by Equation (4) [31].

It is worth noting that as long as a simple model is used, which implies that the 7F term splitting into multiplets is caused solely by the spin-orbit coupling, λ should be considered as an “effective” SOC parameter. Such an effective λ absorbs, along with the true SOC, other effects related to the fine level structure due to the LF. In fact, it is the effective parameter, λ , that is usually found by empirical analyses of magnetic or spectroscopic data obtained for Eu(III) complexes.

3. Results and Discussion

3.1. Synthetic Aspects

As can be seen in Scheme 1, the paramagnetic tripod (a) and its diamagnetic relatives (b,c) have a similar organic molecule organization. Formally, Rad can be classified as a methane derivative, like the other two tripodal ligands, since, for all three molecules, the bridgehead atom is an sp^3 carbon. In addition, despite the difference in the donor atoms on the “legs” of the paramagnetic tripod (oxygen atom from the nitroxyl group instead of pyrazole nitrogen), Rad also forms three six-membered chelate cycles when coordinated.

Upon the coordination of the tris(pyrazol-1-yl)methanes (neutral tripods), anionic ligands are required to compensate for the positive charge of the central atom [32,33], in contrast to their negatively charged congeners, tris(pyrazol-1-yl)borates (TPBs), which form the neutral complexes $\text{Ln}^{\text{III}}(\text{TPB})_3$ [34–38] and $\text{Ln}^{\text{II}}(\text{TPB})_2$ [39–41].

The interaction of $\text{Eu}(\text{NO}_3)_3 \cdot 5\text{H}_2\text{O}$ with a tripodal ligand in a 1:1 ratio in an acetonitrile solution leads to the formation of an aqua complex, $[\text{Eu}(\text{HCPz}_3)(\text{NO}_3)_3\text{H}_2\text{O}] \cdot 2\text{MeCN}$ (**1**), when reacting with unsubstituted trispyrazolylmethane tripod, (HCPz₃), and the water-free nitrate compound, $[\text{Eu}(\text{HC}(\text{Pz}^{\text{Me}}_2)_3)(\text{NO}_3)_3] \cdot \text{MeCN}$ (**2**), upon the coordination of the methylated congener—tris(3,5-dimethyl-1-pyrazolyl)methane. The absence of an aqua-ligand in **2** is most likely due to the steric hindrance of the Pz^{Me}_2 -tripod. It is worth noting that, for the chloride analogue, $[\text{Ln}(\text{HC}(\text{Pz}^{\text{Me}}_2)_3)\text{Cl}_3] \cdot 2\text{MeCN}$, no entry of water molecules into the coordination sphere was also detected upon the reaction in acetonitrile under normal conditions [42], whereas the interaction of hydrated salt, $\text{EuCl}_3 \cdot 6\text{H}_2\text{O}$, with HCPz₃ in tetrahydrofuran (THF) results in the six-aqua complex, $[\text{Eu}(\text{HC}(\text{Pz})_3(\text{H}_2\text{O})_6)\text{Cl}_3]$ [25].

The seven-coordinate mono-tripod complexes, $[\text{Ln}(\text{HC}(\text{Pz}^{\text{Me}}_2)_3)(\text{OTf})_3\text{THF}]$, where $\text{Ln} = \text{Y}, \text{Ho}, \text{Dy}$ were formed in a dry and inert tetrahydrofuran medium [32]. In open air, the reaction in acetonitrile media of $\text{Eu}(\text{OTf})_3$ and HCPz₃ in a 1:1 ratio results in the dimerized entity $[\text{Eu}(\text{HCPz}_3)\text{H}_2\text{O}(\text{OTf})_3]_2$ (**3**), in which the Eu ions are also seven-coordinate. The crystals of **3** contain the acetonitrile and ether solvate molecules, which escape easily during storage. Interestingly, upon using unsubstituted anionic hydro-tris(pyrazolyl)borate (HBPz₃) in THF under an inert atmosphere, the dimeric species $[\text{Ln}(\text{HBPz}_3)_2(\text{OTf})_3]_2$ were also obtained for Y, Eu, in which the two triflates are bridging. In contrast, the molecular complexes of Gd and Yb are monomeric THF adducts, $[\text{Ln}(\text{HBPz}_3)_2(\text{OTf})_3]$ [43].

3.2. Description of the Crystal Structures of 1–3

A summary of the crystallographic data and the structure refinement is given in Table S1 (Supplementary Materials). As established through an X-ray diffraction experiment, the mononuclear compounds crystallize in the following space groups: $P\bar{1}$, $I2/c$, and $P2_1/n$ for **1**, **1a**, and **2**, respectively, as well as the binuclear species **3** in $P2_1/c$. In all compounds, each europium ion is capped with one neutral tripodal ligand. Among the structurally studied heteroleptic complexes, only **1a** does not have solvate molecules; **1** differs from **1a** by the presence of solvate acetonitrile molecules in its crystal structure. In both compounds, the europium center has a coordination number of ten, comprising three nitrogens of trispyrazolylmethane, six oxygens of bidentate nitrate anions, and one aqua–oxygen; see Figure 1.

The Eu–N distances of **1** are in the range of 2.5810(12) to 2.5932(12) Å, which are somewhat larger than those for nitrates (2.4846(10)–2.5687(11) Å), the length of the Eu–O_{aqua} bond of 2.4191(11) Å being the shortest one (Table 1). The same tendency is observed for other compounds. However, compound **2** has the most compact coordination environment and contains a solvated acetonitrile molecule (Figure 2a). According to the ten-coordinate polyhedrons analysis using the SHAPE program [44], the geometry of the lanthanide site in **1** and **1a** can be best described as a sphenocorona (C_{2v}), while for the nine-coordinate environment of **2**, a spherical tricapped trigonal prism (D_{3h}) is more acceptable (Table S2, Supplementary Materials).

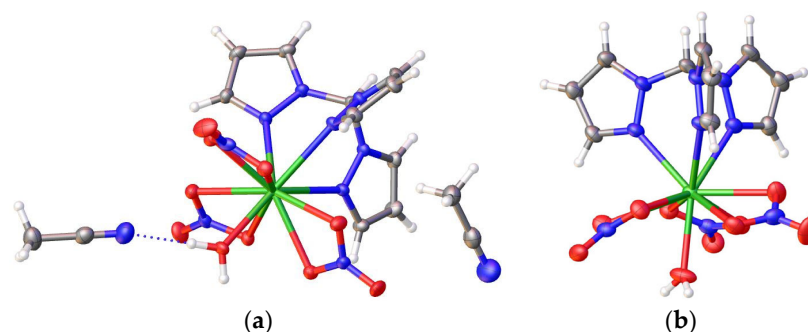


Figure 1. The asymmetric units in the crystal structure of (a) $[\text{Eu}(\text{HCPz}_3)(\text{NO}_3)_3\text{H}_2\text{O}] \cdot 2\text{MeCN}$ (**1**) and (b) $[\text{Eu}(\text{HCPz}_3)(\text{NO}_3)_3\text{H}_2\text{O}]$ (**1a**).

Table 1. The coordination polyhedron bond and Eu–Eu distances (\AA) in the studied compounds.

	1	1a	2	3			
			Eu1¹	Eu2¹			
Eu–N	2.5810 (12)	2.5678 (16)	2.5402 (19)	Eu1–N1	2.520 (8)	Eu2–N7	2.533 (8)
	2.5926 (12)	2.5180 (17)	2.5592 (19)	Eu1–N3	2.537 (8)	Eu2–N9	2.542 (9)
	2.5932 (12)	2.6072 (16)	2.5158 (18)	Eu1–N5	2.552 (8)	Eu2–N11	2.552 (9)
<i>mean</i>	2.5889	2.5643	2.5384		5.36		5.42
Eu–O_{anion}	2.5687 (11)	2.4909 (14)	2.4440 (17)	Eu1–O1	2.378 (6)	Eu2–O11	2.382 (7)
	2.4846 (10)	2.7172 (16)	2.4883 (17)	Eu1–O3 ⁱ	2.404 (6)	Eu2–O14	2.520 (8)
	2.5153 (11)	2.4288 (13)	2.4718 (17)	Eu1–O4	2.376 (6)	Eu2–O17	2.537 (8)
	2.4655 (11)	2.4983 (15)	2.4465 (17)	Eu1–O7	2.334 (6)	Eu2–O19 ⁱⁱ	2.552 (8)
	2.5234 (11)	2.5306 (15)	2.4674 (17)	<i>mean</i>	2.373	<i>mean</i>	2.498
<i>mean</i>	2.5005 (11)	2.5199 (15)	2.4514 (17)				
Eu–O_{aqua}	2.4191 (11)	2.4237 (15)		Eu1–O10	2.382 (7)	Eu2–O20	2.360 (8)
Eu–Eu	6.151	6.646	8.931		6.137		6.073

¹ Symmetry codes for compound **3**: (i) $-x + 3, -y + 2, -z + 2$; (ii) $-x + 2, -y + 2, -z + 2$.

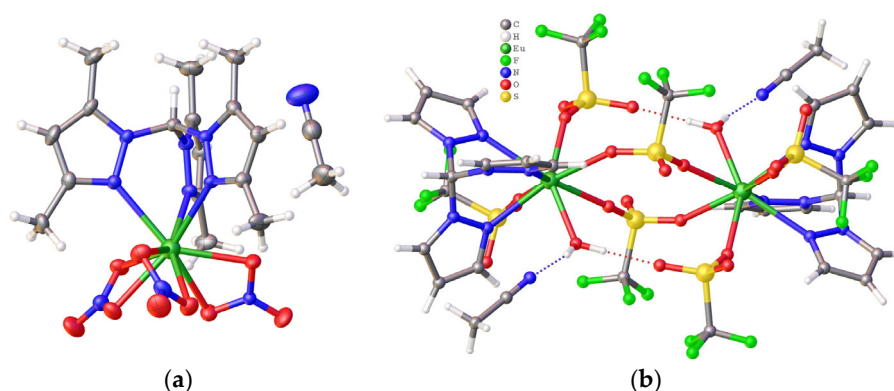


Figure 2. (a) An asymmetric unit in the crystal structure of $[\text{Eu}(\text{HC}(\text{Pz}^{\text{Me}_2})_3)(\text{NO}_3)_3] \cdot \text{MeCN}$ (**2**); (b) the dimer organization for the Eu01 site in the crystal structure of $[\text{Eu}(\text{HCPz}_3)\text{H}_2\text{O}(\text{CF}_3\text{SO}_3)_3]_2$ (**3**).

Among all studied complexes, the most intriguing is the molecular structure of **3**, in which there are two independent Eu^{3+} sites with a coordination number of eight (Figure S1), which is composed of three tripod nitrogens, two μ_2 -oxygens of bridging triflates, two oxygens from monodentate anions, and one aqua–oxygen. A duplication of the corresponding independent parts via an inversion center gives two different dimeric molecules, one of which is shown in Figure 2b. In addition to the two bidentate triflates, each binuclear entity is supported by two water–triflate hydrogen bonds, which are in a plane perpendicular to that in which the bridging anions are located, thus forming a *Chinese lantern* structure.

The stereochemical analysis indicates that the coordination polyhedron for the two Eu sites corresponds well to a square antiprism (D_{4d}) (Figure S2, Table S2, Supplementary Materials). Nevertheless, despite the similar polyhedron geometry, the two Eu sites differ quite significantly in the Eu–ligand bond lengths, which are, on average, shorter for Eu1 (Table 1).

A crystal packing analysis shows that the shortest Eu–Eu distances are in the range of 6.073–8.931 Å (Table 1). These distances have an intermolecular character only for **2**, in which no hydrogen bonds were detected, while **3** is a binuclear species, and the compounds **1** and **1a** are dimerized due to the formation of a double hydrogen bond (Figure S3, Supplementary Materials). The lengths of the shortest intermolecular contacts between a tripod and anionic ligand, $\text{CH}^{\text{L}} \cdots \text{O}_{\text{anion}}$, are 3.281, 3.245, 3.334, and 3.325 Å for **1**, **1a**, **2**, and **3**, respectively.

3.3. Magnetic Behavior of The Complexes

The experimental *dc* magnetic susceptibility data for complexes **1–3**, measured in the temperature range from 1.77 to 300 K at the applied magnetic field $H = 1$ kOe, are shown as $\chi_M T$ vs. T plots in Figure 3 (where χ_M is the molar magnetic susceptibility corrected for the diamagnetic contribution). As expected, due to the thermal depopulation of the excited levels with non-zero J values, $\chi_M T$ gradually decreases with cooling and tends towards a value that is very close to zero as the temperature approaches absolute zero. The $\chi_M T$ values at low and room temperature for all complexes are summarized in Table 2. Below ≈ 100 K, $\chi_M T$ varies almost linearly with T (Figure 3), implying that χ_M is nearly temperature-independent at low T . Indeed, presented in Figure S4, the $\chi_M(T)$ dependences exhibit a smooth growth upon cooling and tend to saturate, and form a plateau below ~ 100 K. A small increase in χ_M at the lowest temperatures is due to the inevitable presence of an Eu^{2+} admixture (at a level of 0.01–0.017 at.%) or other rare-earth impurity ions possessing a paramagnetic ground state. The subtraction of this impurity contribution gives the intrinsic temperature-independent magnetic susceptibility of Eu^{3+} ions.

The temperature dependences of $\chi_M T$ in Figure 3 can be analyzed using the Van Vleck approximation (4), and assuming a simplified electronic structure of a Eu^{3+} ion composed of seven multiplets with energies of $E(J) = \lambda J(J + 1)/2$ [29]. The least squares fitting using Equation (4) with effective λ as the only adjustable parameter (dashed blue lines in Figure 3) results in the λ values of ≈ 383 – 406 cm^{-1} for **1–3** (Table 2)—values typical for Eu^{3+} molecular compounds. A common feature of all these fits is that they underestimate the $\chi_M T$ values in the low-temperature region, where χ_M exhibits a plateau. As was discussed in Section 2, this feature is quite expected because Equation (4) does not take into account the zero-field splitting of the excited multiplets with $J \neq 0$. The latter inevitably reduces the energy difference between the ground-state $J = 0$ level and the lowest-energy sublevel of the $J = 1$ multiplet, E_1 [29–31]. In the case of strong zero-field splitting, E_1 may be significantly smaller than λ , thereby providing the low- T magnetic susceptibility to be much larger than $\chi_{LT} = 8N\beta^2/\lambda$, predicted using Equation (4) [31].

In the entire available temperature range, the field dependences of the magnetization, $M(H)$, demonstrate an almost perfect linear behavior (Figure 4). However, the magnetization value is 2–3 orders of magnitude lower than that of other rare-earth ions with a $J \neq 0$ ground state. Even at the lowest temperature, $T = 1.77$ K, the magnetization at $H = 10$ kOe reaches only $\approx 0.01 \mu_B$ per Eu^{3+} ion. These features are common to many other europium(III) complexes with diamagnetic ligands presented in Table 2.

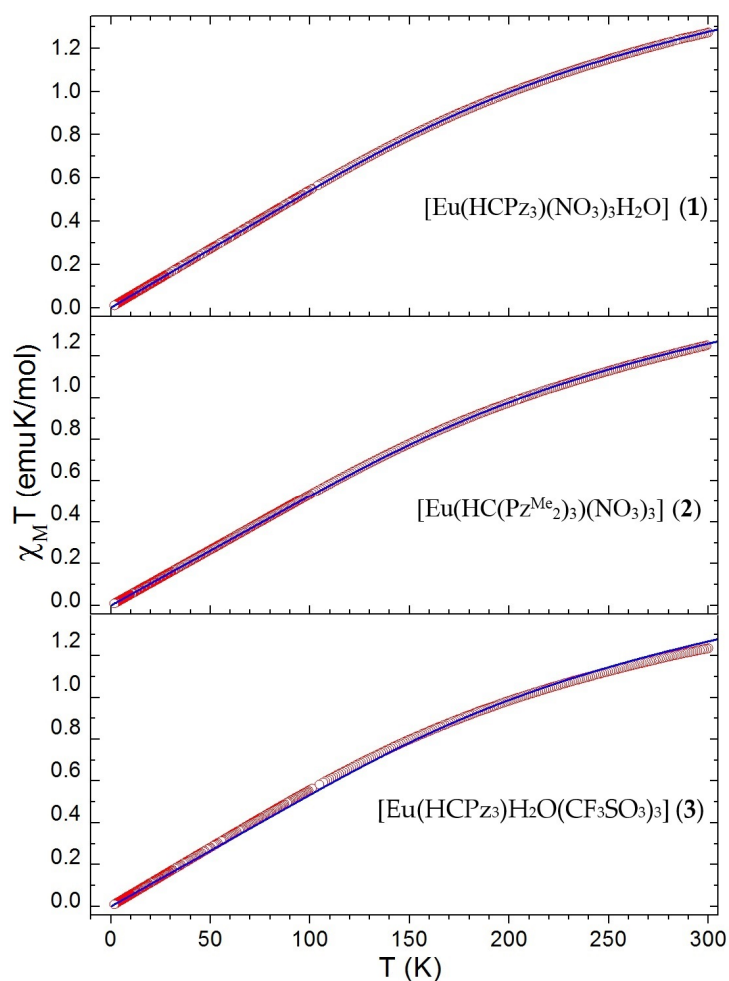


Figure 3. The $\chi_M T$ versus T data (\circ) measured at the applied magnetic field $H = 1$ kOe. The blue lines show the best fits to the data of Equation (4), with the spin–orbit coupling parameter, λ , being the only adjustable parameter; the resulting values of λ are presented in Table 2.

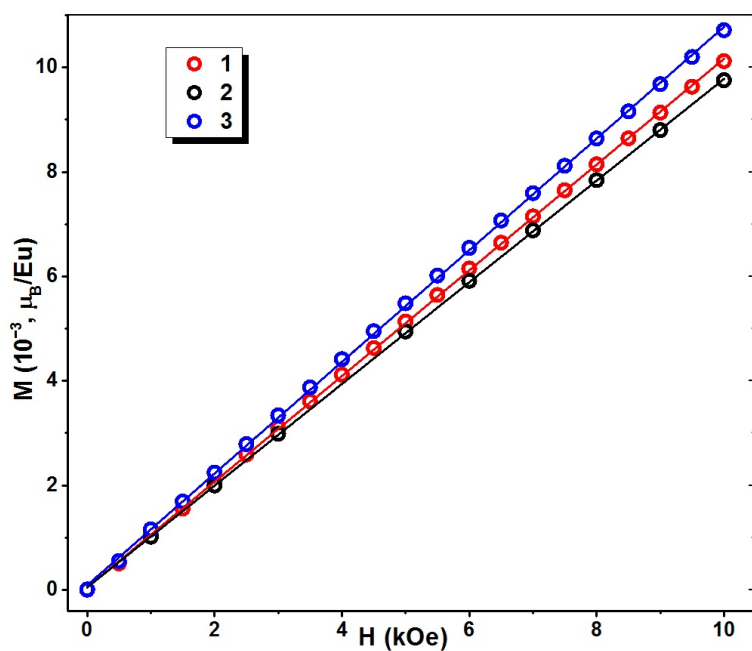


Figure 4. Field dependences of the magnetization measured for 1–3 at $T = 1.77$ K.

Table 2. Magnetic parameters for europium(III) molecular compounds.

Compound	$\chi_M T$ (emu·K/mol)	λ (cm ⁻¹) ^a	R ^b	Reference
Free Eu ³⁺	2 K 0	300 K 1.280		
1	0.0113	1.228	1.02×10^{-4}	[26,45,46] this work
2	0.0114	1.251	4.10×10^{-5}	this work
3 /Eu	0.0120	1.255	3.26×10^{-4}	this work
[Eu ₂ (L ¹) ₆ (H ₂ O) ₄] _n /Eu	0.025	1.325		[47]
[Eu ₂ (tzf) ₃ (H ₂ O) ₆] _n /Eu	0.020	1.388	2.7×10^{-4}	[48]
[Eu ₂ L ² ₆ Pen ₂ (H ₂ O) ₂]/Eu			3.1×10^{-4}	[49]
[EuL ³ (H ₂ O) ₂ SO ₄] _n			4.28×10^{-4}	[50]
[EuL ⁴ ₃ (CH ₃ OH) ₃] _n			9.65×10^{-5}	[51]
[Eu ₂ (Hpcpa) ₃ (H ₂ O) ₅] _n	sap	1.2	2.2×10^{-5}	[52]
[Eu(HL ^{Cl}) ₄ (dmso)] ⁻		1.37	4.1×10^{-5}	[53]
[Eu(HL ^F) ₄ (dmso)] ⁻		1.37	2.1×10^{-5}	[53]
[EuL ⁵ ₂ (H ₂ O) ₄](ClO ₄) ₃]			7.0×10^{-4}	[29]
[Eu(^{trip} PBAP) ₃]				[6]
[EuL ⁶ PhCOO](ClO ₄) ₂	0.015	1.30		[54]
[Eu(Nitrone) ₂ (NO ₃) ₃]		1.25		[15]
[Eu(HBPz ₃) ₂ Trp]	0.037	1.48		[22]
[Eu(hfac) ₃ NN ^e]	0.192	1.946	2.0×10^{-3}	[19]
[Eu(OEP) ²⁻ (OEP) ⁻]	0.208	1.575		[20]
[Eu ^{III} (AP ²⁻)(ISQ) ⁻]	0.252	1.834		[21]
[Eu(HBPz ₃) ₂ SQ]	0.28	1.59		[22]
[Eu(hfac) ₃ NN ₂] ^{SMMTb}	0.035	2.24		[12]
[Eu(hfac) ₃ ^{PhOMe} NN ₂]	0.11	1.89		[13]
[Eu(hfac) ₃ NN ₂]	0.12	1.98		[14]
[EuNN ^{trz} ₂ (NO ₃) ₃]	0.24	1.93		[15]
[Eu(hfac) ₃ NN ₂]	0.419	3.09		[16]
[Eu(hfac) ₃ NN ₂]		2.38		[17]
[Eu(hfac) ₃ NN ₂]		2.12		[18]
[EuRad ₂ (OTf) ₃]	0.348	1.78		[11]
[Eu(hfac) ₃ NN ^{Et}] _n	0.89	1.9		[55]
[Eu(hfac) ₃ NN] _n		1.88	1.47×10^{-4}	[56]
[Eu ₂ (acac) ₄ ^{PhO} NN ₂]	0.66	3.47	2.67×10^{-5}	[57]
[NN ₄ CuL ₂ (Eu(hfac) ₃) ₃]	0.38	5.78	1.8×10^{-3}	[58]

^a Spin-orbit coupling parameter; ^b agreement factor; ^c found from the optic data at 77 K; ^d found from the optic data at RT; ^e NN—nitronyl nitroxide radical ligand.

3.4. Spin-Orbit Coupling Parameter Analysis

As can be seen from Table 2, the values of the coefficients of agreement (R) indicate the validity of the chosen theoretical model for all compounds studied by us. However, for the nitrate-containing complexes, **1** and **2**, this agreement is better compared to **3**. This is most likely due to the significant difference in the splitting of Eu³⁺ excited levels (especially of the ⁷F₁ state) under the action of the ligand field. Indeed, despite approximately the same set of donor atoms—nitrogens from a tripodal ligand and oxygens from the anion ligands—the latter, in compound **3**, have a pronounced electron-withdrawing character, whereas nitrate ligands possess this property to a lesser extent, which is confirmed by the difference in Eu–O bond lengths (Table 1). In addition, despite the presence of two different europium sites in **3**, the symmetry of their local environment (*D*_{4d}) is higher than that of the other two: *C*_{2v} for **1** and *D*_{3h} for **2** (Table S2, Supplementary Materials). Based on the above, it is not surprising that fitting the experimental curve with the model with only one variable, λ , leads, in the case of compound **3**, to a less accurate result compared to **1** and **2**. Moreover, for a more precise theoretical description, it might be necessary to take into account the interaction between Eu ions by introducing into the model the coupling constant, j_{Eu-Eu} . However, without additional experimental data such as the luminescence spectra, the use of five independent variables would lead to overparametrization.

According to the agreement coefficients, R , the fitting quality achieved is sufficient to conclude that the spin–orbit coupling parameters, λ , in **1** and **2** are different (by $\sim 10 \text{ cm}^{-1}$). Indeed, despite the same type of tripod and anionic ligands, the coordination environment of the Eu site is significantly different for **1** and **2**, due to the presence of one water molecule in the former. Therefore, **1** has a lower symmetry of the coordination polyhedron compared to **2**, which leads to a smaller splitting of the excited levels in the crystal field. This fact is consistent with the higher value of λ : 406 for **1** vs. 396 cm^{-1} for **2**.

4. Experimental Section

4.1. Materials and Physical Measurements

$\text{Ln}(\text{CF}_3\text{SO})_3$ salts (Thermo Fisher GmbH, Kandel, Germany) were purchased from Alfa Aesar. $\text{Eu}(\text{NO}_3)_3 \cdot 6\text{H}_2\text{O}$ was prepared upon the dissolution of the corresponding Eu_2O_3 in diluted HNO_3 at 50 °C, followed by crystallization during the slow evaporation of the reaction mixture. Solvents of the reagent grade (EKOS-1, Moscow, Russia) were distilled prior to use. The complexes were synthesized under aerobic conditions. Elemental (C, H, N, S) analyses were carried out using standard methods with a Euro-Vector 3000 analyzer (Eurovector, Redavalle, Italy).

Magnetic measurements were performed using a MPMS-XL SQUID magnetometer (Quantum Design, San Diego, CA, USA) in the temperature range of 1.77–300 K at magnetic fields of up to 10 kOe. In order to determine the paramagnetic component of the molar magnetic susceptibility, $\chi_M T(T)$, the temperature-independent diamagnetic contribution, χ_d , and a possible magnetization of ferromagnetic micro-impurities, $\chi_{FM}(T)$, were evaluated and subtracted from the measured values of the total molar susceptibility, $\chi = M/H$. The diamagnetic intrinsic contributions of the compounds, χ_d , were estimated using the Pascal's constants [59]. Fourier transform infrared (FTIR) spectra were measured in KBr pellets with a Perkin–Elmer System 2000 FTIR spectrometer (Perkin Elmer, Waltham, MA, USA) in the 4000–400 cm^{-1} range.

4.2. Single-Crystal XRD Experiment and Data Refinement Details

Single-crystal XRD data for crystals of the compounds were collected at 150 K with a Bruker D8 Venture diffractometer (Bruker, Karlsruhe, Germany) (0.5° ω - and φ -scans, fixed- χ three circle goniometer, CMOS PHOTON III detector, I μ S 3.0 micro-focus source, focusing Montel mirrors, $\lambda = 0.71073 \text{ \AA}$ MoK α radiation, N $_2$ -flow thermostat). Data reduction was performed routinely via APEX 3 suite [60]. The crystal structures were solved using the Bruker SHELXTL (version 2018/3) [61] and were refined using ShelXL [62] programs assisted by Olex2 GUI (Version 1.3.0) [63]. Atomic displacements for non-hydrogen atoms were refined in harmonic anisotropic approximation, with the exception for the partially occupied diethyl ether molecule in **3**. Hydrogen atoms were located geometrically, with the exception of those in water molecules in **1** and **1a**, which were refined freely with the restraints on the O–H bond. All hydrogens were placed in geometrically idealized positions, and were refined in a riding model. The crystals of compound **3** tend to form twins; as a result, the quality of the structure is lower than that of the others. The structures of the complexes were deposited to the Cambridge Crystallographic Data Centre (CCDC) as a supplementary publication, No. 2285187–2285190.

4.3. Synthesis of the Complexes

$[\text{Eu}(\text{HCPz}_3)(\text{NO}_3)_3\text{H}_2\text{O}] \cdot 2\text{MeCN}$ (**1**): A solution of trispyrazolylmethane (64.5 mg, 0.3 mmol) in acetonitrile (0.5 mL) was added dropwise to a stirred warm solution of $\text{Eu}(\text{NO}_3)_3(\text{H}_2\text{O})_5$ (128 mg, 0.3 mmol) in acetonitrile (0.5 mL). The next day, the crystalline, colorless precipitate was filtered, washed with a small amount of acetonitrile and Et_2O , and air-dried. Yield: 158 mg (81%) (652.32 g/mol). The storage of the compound resulted in unsolvated **1**. Anal. calcd. (%) for $\text{C}_{10}\text{H}_{12}\text{EuN}_9\text{O}_{10}$: C, 21.02; H, 2.12; N, 22.07. Found: C, 21.1; H, 2.0; N, 22.1. IR (KBr): ν (cm^{-1}) 3423 (m), 3115 (m), 3111 (m), 2505 (m), 2427 (sh), 1507 (s), 1384 (s), 1317 (s), 1285 (s), 1230 (m), 1148 (s), 1186 (s), 1148 (s), 1136 (s), 1119 (m),

1042 (m), 1028 (m), 1009 (m), 981 (m), 963 (m), 904 (m), 876 (m), 730 (s), 723 (s), 672 (s), 664 (s), 651 (m).

$[Eu(HCPz_3)(NO_3)_3H_2O]$ (**1a**): The mother liquor and flushing liquids that remain after the synthesis of **1** were combined and evaporated to dryness. The white powder that formed (30 mg) was dissolved in hot dry acetonitrile (2 mL). After filtration, the filtrate was left in a refrigerator at a temperature of 4 C for one week. The colorless crystals were filtered, rinsed with a small amount of cold acetonitrile, and air-dried. Yield: 17 mg (570.22 g/mol); Anal. calcd. (%) for $C_{10}H_{12}EuN_9O_{10}$: C, 21.02; H, 2.12; N, 22.07. Found: C, 21.2; H, 2.1; N, 22.0. I. IR (KBr) is similar to that of **1**.

$[Eu(HC(Pz^{Me}_2)_3)(NO_3)_3] \cdot MeCN$ (**2**): To a stirred and hot solution of the metal salt of $Eu(NO_3)_3(H_2O)_5$ (84 mg, 0.2 mmol) in acetonitrile (1.5 mL) solid tris(3,5-dimethyl-1-pyrazolyl)methane (60 mg, 0.2 mmol) was gradually added under heating. The solution was filtered and kept at room temperature overnight, and then the resulting colorless crystalline solid was sucked off, washed twice with cold acetonitrile, and air-dried. Yield: 112 mg (84%) (677.41 g/mol). The storage of the compound resulted in unsolvated **2**. Anal. calcd. (%) for $C_{16}H_{22}EuN_9O_9$: C, 30.14; H, 3.48; N, 19.65. Found C, 30.2; H, 3.3; N, 19.65. IR (KBr) ν (cm^{-1}): 487 (m); 636 (w); 707 (s); 746 (s); 802 (m); 811 (s); 822 (w); 836 (m); 859 (s); 864 (s); 906 (s); 983 (m); 1024 (s); 1042 (s); 1109 (m); 1153 (w); 1169 (w); 1276 (s); 1304 (s); 1417 (m); 1515 (s); 1530 (m); 1570 (s); 1732 (w); 1771 (w); 1977 (w); 2043 (w); 2268 (m); 2292 (w); 2533 (w).

$[Eu(HCPz_3)H_2O(CF_3SO_3)_3]_2 \cdot 2MeCN \cdot 0.73Et_2O$ (**3**): A solution of trispyrazolylmethane (54 mg, 0.25 mmol) in acetonitrile (1 mL) was added dropwise to a stirred solution of $Eu(CF_3SO_3)_3$ (150 mg, 0.25 mmol) in acetonitrile (2 mL). The reaction mixture was halved via heating (65 C) and slowly cooled to room temperature, and then left undisturbed overnight in a closed vessel with a few drops of Et_2O . The crystalline, colorless solid was filtered, washed with a small amount of acetonitrile and Et_2O , and air-dried. Yield: 209 mg (45%) $C_{32.9}H_{37.24}Eu_2F_{18}N_{14}O_{20.73}S_6$ (1798.66 g/mol). The storage of the compound resulted in unsolvated **3**. Anal. calcd. (%) for $C_{26}H_{24}Eu_2F_{18}S_6N_{12}O_{20}$ (1662.8 g/mol): Anal. calcd. (%): C, 18.78, H, 1.45, N, 10.11; S, 11.7; found: C, 18.6, H, 1.6, N, 10.0; S, 11.5. IR (KBr) ν (cm^{-1}): 3140 (w); 3130 (w); 1578 (m); 1549 (m); 1527 (m); 1409 (m); 1292 (s); 1200 (s); 1166 (s); 1110 (m); 1094 (m); 1029 (m); 960 (m); 920 (m); 889 (m); 857 (m); 824 (m); 810 (m); 755 (s); 722 (m); 638 (s); 597 (m); 574 (m); 517 (m); 410 (w); 389 (w); 351 (w).

5. Conclusions and Perspectives

In this work, europium(III) complexes involving one neutral tripodal ligand with a predictable mode of coordination have been synthesized and structurally studied. In the case of unsubstituted trispyrazolylmethane and hydrated europium nitrate, the complex $[Eu(HCPz_3)(NO_3)_3H_2O]$ has been obtained upon crystallization, of which, from acetonitrile, two different solid phases can be formed, both with (**1**) and without (**1a**) solvated molecules in the crystal. In the case of europium(III) trifluoromethylsulfonate, the dimeric coordination compound $[Eu(HCPz_3)H_2O(CF_3SO_3)_3]_2$ (**3**) is formed, in which the two anionic ligands are bidentate, and two of the four monodentate triflates form short hydrogen bonds with the aqua ligand of the neighboring Eu center, thus forming a *Chinese lantern* structure. The replacement of tripod $HCPz_3$ by its methylated analogue $HC(Pz^{Me}_2)_3$ leads to the formation of a nine-coordination complex, $[Eu(HC(Pz^{Me}_2)_3)(NO_3)_3]$ (**2**), which does not include an aqua ligand, unlike the complexes of the unsubstituted congener.

For compounds **1–3**, *dc* magnetic measurements were performed in the range of $2 \div 300$ K at $H = 1000$ and $10,000$ Oe. Based on these data, and using the theoretical modeling of the temperature dependences of magnetic susceptibility, the spin–orbit coupling parameter, λ , was obtained, which varies in the range of $383 \div 406$ cm^{-1} , only slightly differing from that for the free Eu^{3+} ions.

In the absence of analytical models accounting for strong spin–orbit coupling in Eu^{3+} complexes with paramagnetic ligands, alternative approaches are needed to determine the nature and magnitude of the exchange coupling between paramagnetic centers in

such complicated systems. The earlier proposed solution, based on subtraction from the experimental dependence of the magnetic susceptibility, $\chi_M(T)$, for a series of lanthanide complexes with radicals [15,23], the same dependence of the model compound of the corresponding Ln with a diamagnetic ligand possessing a similar coordination polyhedron geometry turned out to be particularly effective for $[\text{Ln}(\text{HBPz}_3)_2\text{SQ}]$ [23].

Based on the stereochemical analysis of the coordination environment in compound **2**, it was stated that the complexes $[\text{Ln}(\text{HC}(\text{Pz}^{\text{Me}_2})_3)(\text{NO}_3)_3]$ [42] can be used as a model system for the monoradical complexes $[\text{LnRad}(\text{NO}_3)_3]$, since both types of compounds have the same type of coordination polyhedron (symmetry point group D_{3h}) and very close Ln–donor atom distances. It is quite possible that the neutral ligand $\text{HC}(\text{Pz}^{\text{Me}_2})_3$ can also be used for the synthesis of bis-tripodal complexes, $[\text{Ln}(\text{HC}(\text{Pz}^{\text{Me}_2})_3)_2](\text{anion})_3$, as model systems for biradical compounds with sterically hindered paramagnetic tripods, $[\text{Ln}(\text{Rad})^{\text{Me}_2}](\text{anion})_3$, for which the corresponding ligands are under preparation [64]. As surprising as it may be, the homoleptic Ln^{3+} complexes involving two bulky diamagnetic tripods of type $\text{HC}(\text{Pz}^{\text{Me}_2})_3$ in their composition are still unknown. Consequently, developing methods to synthesize them is a particular challenge.

Supplementary Materials: The following supporting information can be downloaded at <https://www.mdpi.com/article/10.3390/inorganics11100418/s1>: Table S1: Crystal data and structure refinement for the compounds; Figure S1: The asymmetric unit in the crystal structure of $[\text{Eu}(\text{HCPz}_3)_2\text{H}_2\text{O}(\text{CF}_3\text{SO}_3)_3]_2$ (**3**); Figure S2: Square antiprism coordination environment—of Eu^{3+} sites in $[\text{Eu}(\text{HCPz}_3)_2\text{H}_2\text{O}(\text{CF}_3\text{SO}_3)_3]_2$ (**3**) for: (a) around Eu1 central atom, (b) around Eu2 central atom; Table S2: Geometry analysis of the complexes by SHAPE software; Figure S3: Dimerized species in **1** (left) and **1a** (right); Figure S4: The temperature-dependent molar magnetic susceptibility χ_M of **1–3** at a field of 1 kOe (open red circles). Solid green circles show the χ_M data after subtraction of the contribution from Eu(II) impurities (0.01–0.017%).

Author Contributions: Conceptualization, K.E.V. and A.N.L.; methodology, K.E.V.; software, T.S.S.; formal analysis, T.S.S.; investigation, K.E.V. and A.N.L.; resources, K.E.V.; data curation, T.S.S.; writing—original draft preparation, K.E.V.; writing—review and editing, K.E.V. and A.N.L.; visualization, K.E.V. and A.N.L.; supervision, K.E.V.; funding acquisition, K.E.V. All authors have read and agreed to the published version of the manuscript.

Funding: This research was funded by the Russian Science Foundation, Grant No. 23-23-00437, and was partially supported by the Ministry of Science and Higher Education of the Russian Federation (single crystal XRD data collection for the complexes, 121031700313-8).

Data Availability Statement: The CCDC 2285187–2285190 for **1–4** contain the supplementary crystallographic data for this paper, and can be obtained free of charge from The Cambridge Crystallographic Data Centre via <https://www.ccdc.cam.ac.uk/structures/> (accessed on 31 July 2023).

Conflicts of Interest: The authors declare no conflict of interest.

References

1. Yi, X.; Bernot, K.; Pointillart, F.; Poneti, G.; Calvez, G.; Daguebonne, C.; Guillou, O.; Sessoli, R. A Luminescent and Sublimable DyIII-Based Single-Molecule Magnet. *Chem. A Eur. J.* **2012**, *18*, 11379–11387. [[CrossRef](#)] [[PubMed](#)]
2. Marin, R.; Brunet, G.; Murugesu, M. Shining New Light on Multifunctional Lanthanide Single-Molecule Magnets. *Angew. Chem. Int. Ed.* **2021**, *60*, 1728–1746. [[CrossRef](#)] [[PubMed](#)]
3. Suta, M.; Wickleder, C. Synthesis, Spectroscopic Properties and Applications of Divalent Lanthanides Apart from Eu^{2+} . *J. Lumin.* **2019**, *210*, 210–238. [[CrossRef](#)]
4. Morss, L.R. Chapter 122 Comparative Thermochemical and Oxidation-Reduction Properties of Lanthanides and Actinides. In *Handbook on the Physics and Chemistry of Rare Earths*; Elsevier: Amsterdam, The Netherlands, 1994; Volume 18, pp. 239–291, ISBN 0168-1273.
5. Rodrigues, L.C.V.; Hölsä, J.; Brito, H.F.; Maryško, M.; Matos, J.R.; Paturi, P.; Rodrigues, R.V.; Lastusaari, M. Magneto-Optical Studies of Valence Instability in Europium and Terbium Phosphors. *J. Lumin.* **2016**, *170*, 701–706. [[CrossRef](#)]
6. Chen, J.; Carpenter, S.H.; Fetrow, T.V.; Mengell, J.; Kirk, M.L.; Tondreau, A.M. Magnetism Studies of Bis(Acyl)Phosphide-Supported Eu^{3+} and Eu^{2+} Complexes. *Inorg. Chem.* **2022**, *61*, 18466–18475. [[CrossRef](#)] [[PubMed](#)]
7. Evans, W.J. Perspectives in Reductive Lanthanide Chemistry. *Coord. Chem. Rev.* **2000**, *206–207*, 263–283. [[CrossRef](#)]

8. Dolai, M.; Ali, M.; Rajnák, C.; Titiš, J.; Boča, R. Slow Magnetic Relaxation in Cu(II)–Eu(III) and Cu(II)–La(III) Complexes. *New J. Chem.* **2019**, *43*, 12698–12701. [[CrossRef](#)]
9. Wang, J.; Ruan, Z.-Y.; Li, Q.-W.; Chen, Y.-C.; Huang, G.-Z.; Liu, J.-L.; Reta, D.; Chilton, N.F.; Wang, Z.-X.; Tong, M.-L. Slow Magnetic Relaxation in a {EuCu₅} Metallocrown. *Dalt. Trans.* **2019**, *48*, 1686–1692. [[CrossRef](#)]
10. Perfetti, M.; Caneschi, A.; Sukhikh, T.S.; Vostrikova, K.E. Lanthanide Complexes with a Tripodal Nitroxyl Radical Showing Strong Magnetic Coupling. *Inorg. Chem.* **2020**, *59*, 16591–16598. [[CrossRef](#)]
11. Rey, P.; Caneschi, A.; Sukhikh, T.S.; Vostrikova, K.E. Tripodal Oxazolidine-N-Oxyl Diradical Complexes of Dy³⁺ and Eu³⁺. *Inorganics* **2021**, *9*, 91. [[CrossRef](#)]
12. Tretyakov, E.V.; Fokin, S.V.; Zueva, E.M.; Tkacheva, A.O.; Romanenko, G.V.; Bogomyakov, A.S.; Larionov, S.V.; Popov, S.A.; Ovcharenko, V.I. Complexes of Lanthanides with Spin-Labeled Pyrazolylquinoline. *Russ. Chem. Bull.* **2014**, *63*, 1459–1464. [[CrossRef](#)]
13. Wang, X.; Li, Y.; Hu, P.; Wang, J.; Li, L. Slow Magnetic Relaxation and Field-Induced Metamagnetism in Nitronyl Nitroxide-Dy(III) Magnetic Chains. *Dalt. Trans.* **2015**, *44*, 4560–4567. [[CrossRef](#)] [[PubMed](#)]
14. Wang, Y.; Fan, Z.; Yin, X.; Wang, S.; Yang, S.; Zhang, J.; Geng, L.; Shi, S. Structure and Magnetic Investigation of a Series of Rare Earth Heterospin Monometallic Compounds of Nitronyl Nitroxide Radical. *Z. Für Anorg. Und Allg. Chem.* **2016**, *642*, 148–154. [[CrossRef](#)]
15. Kahn, M.L.; Sutter, J.-P.; Golhen, S.; Guionneau, P.; Ouahab, L.; Kahn, O.; Chasseau, D. Systematic Investigation of the Nature of the Coupling between a Ln(III) Ion (Ln = Ce(III) to Dy(III)) and Its Aminoxyl Radical Ligands. Structural and Magnetic Characteristics of a Series of {Ln(Radical)₂} Compounds and the Related {Ln(Nitronyl)₂} Derivat. *J. Am. Chem. Soc.* **2000**, *122*, 3413–3421. [[CrossRef](#)]
16. Lv, X.-H.; Yang, S.-L.; Li, Y.-X.; Zhang, C.-X.; Wang, Q.-L. A Family of Lanthanide Compounds Based on Nitronyl Nitroxide Radicals: Synthesis, Structure, Magnetic and Fluorescence Properties. *RSC Adv.* **2017**, *7*, 38179–38186. [[CrossRef](#)]
17. Fan, Z.; Hou, Y.-F.; Wang, S.-P.; Yang, S.-T.; Zhang, J.-J.; Shi, S.-K.; Geng, L.-N. Synthesis, Crystal Structure, and Magnetic Property of New Trispin Ln(III)-Nitronyl Nitroxide Complexes. *Helv. Chim. Acta* **2016**, *99*, 732–741. [[CrossRef](#)]
18. Wang, Y.-L.; Gao, Y.-Y.; Ma, Y.; Wang, Q.-L.; Li, L.-C.; Liao, D.-Z. Syntheses, Crystal Structures, Magnetic and Luminescence Properties of Five Novel Lanthanide Complexes of Nitronyl Nitroxide Radical. *J. Solid State Chem.* **2013**, *202*, 276–281. [[CrossRef](#)]
19. Xu, J.-X.; Ma, Y.; Liao, D.; Xu, G.-F.; Tang, J.; Wang, C.; Zhou, N.; Yan, S.-P.; Cheng, P.; Li, L.-C. Four New Lanthanide–Nitronyl Nitroxide (Ln^{III} = Pr^{III}, Sm^{III}, Eu^{III}, Tm^{III}) Complexes and a Tb^{III} Complex Exhibiting Single-Molecule Magnet Behavior. *Inorg. Chem.* **2009**, *48*, 8890–8896. [[CrossRef](#)]
20. Buchler, J.W.; De Cian, A.; Fischer, J.; Kihn-Botulinski, M.; Weiss, R. Metal Complexes with Tetrapyrrole Ligands. 46. Europium(III) Bis(Octaethylporphyrinate), a Lanthanoid Porphyrin Sandwich with Porphyrin Rings in Different Oxidation States, and Dieuropium(III) Tris(Octaethylporphyrinate). *Inorg. Chem.* **1988**, *27*, 339–345. [[CrossRef](#)]
21. Klementyeva, S.V.; Gritsan, N.P.; Khusniyarov, M.M.; Witt, A.; Dmitriev, A.A.; Suturina, E.A.; Hill, N.D.D.; Roemmele, T.L.; Gamer, M.T.; Boeré, R.T.; et al. The First Lanthanide Complexes with a Redox-Active Sulfur Diimide Ligand: Synthesis and Characterization of [LnCp*₂(RN=)S], Ln=Sm, Eu, Yb; R=SiMe₃. *Chem. A Eur. J.* **2017**, *23*, 1278–1290. [[CrossRef](#)]
22. Caneschi, A.; Dei, A.; Gatteschi, D.; Pousereau, S.; Sorace, L. Antiferromagnetic Coupling between Rare Earth Ions and Semiquinones in a Series of 1:1 Complexes. *Dalt. Trans.* **2004**, *7*, 1048–1055. [[CrossRef](#)] [[PubMed](#)]
23. Dei, A.; Gatteschi, D.; Pécaut, J.; Pousereau, S.; Sorace, L.; Vostrikova, K. Crystal Field and Exchange Effects in Rare Earth Semiquinone Complexes. *Comptes Rendus L'academie Sci. Ser. IIC Chem.* **2001**, *4*, 135–141. [[CrossRef](#)]
24. Gaft, M.; Reisfeld, R.; Panczer, G. *Modern Luminescence Spectroscopy of Minerals and Materials*; Springer: Berlin/Heidelberg, Germany, 2005; ISBN 3-540-21918-8.
25. Machado, K.; Mukhopadhyay, S.; Videira, R.A.; Mishra, J.; Mobin, S.M.; Mishra, G.S. Polymer Encapsulated Scorpionate Eu 3+ Complexes as Novel Hybrid Materials for High Performance Luminescence Applications. *RSC Adv.* **2015**, *5*, 35675–35682. [[CrossRef](#)]
26. Binnemans, K. Interpretation of Europium(III) Spectra. *Coord. Chem. Rev.* **2015**, *295*, 1–45. [[CrossRef](#)]
27. Bünzli, J.-C.G. On the Design of Highly Luminescent Lanthanide Complexes. *Coord. Chem. Rev.* **2015**, *293–294*, 19–47. [[CrossRef](#)]
28. Sorace, L.; Gatteschi, D. Electronic Structure and Magnetic Properties of Lanthanide Molecular Complexes. In *Lanthanides and Actinides in Molecular Magnetism*; Wiley-VCH Verlag GmbH & Co. KGaA: Weinheim, Germany, 2015; pp. 1–26.
29. Andruh, M.; Bakalbassis, E.; Kahn, O.; Trombe, J.C.; Porcher, P. Structure, Spectroscopic and Magnetic Properties of Rare Earth Metal(III) Derivatives with the 2-Formyl-4-Methyl-6-(N-(2-Pyridylethyl)Formimidoyl)Phenol Ligand. *Inorg. Chem.* **1993**, *32*, 1616–1622. [[CrossRef](#)]
30. Huang, J.; Lorigs, J.; Porcher, P.; Teste de Sagey, G.; Caro, P.; Levy-Clement, C. Crystal Field Effect and Paramagnetic Susceptibility of Na₅Eu(MoO₄)₄ and Na₅Eu(WO₄)₄. *J. Chem. Phys.* **1984**, *80*, 6204–6209. [[CrossRef](#)]
31. Caro, P.; Porcher, P. The Paramagnetic Susceptibility of C-Type Europium Sesquioxide. *J. Magn. Magn. Mater.* **1986**, *58*, 61–66. [[CrossRef](#)]
32. Sella, A.; Brown, S.E.; Steed, J.W.; Tocher, D.A. Synthesis and Solid-State Structures of Pyrazolylmethane Complexes of the Rare Earths. *Inorg. Chem.* **2007**, *46*, 1856–1864. [[CrossRef](#)]
33. Chen, S.-J.; Li, Y.-Z.; Chen, X.-T.; Shi, Y.-J.; You, X.-Z. Tetrabutylammonium Tetrakis(Nitrato-κ₂O,O′)[1,3,5-Tris(Pyrazolyl)Methane-κ₃N]Cerate(III). *Acta Crystallogr. Sect. E Struct. Rep. Online* **2002**, *58*, m753–m755. [[CrossRef](#)]

34. Bagnall, K.W.; Tempest, A.C.; Takats, J.; Masino, A.P. Lanthanoid Poly(Pyrazol-1-Yl) Borate Complexes. *Inorg. Nucl. Chem. Lett.* **1976**, *12*, 555–557. [[CrossRef](#)]
35. Stainer, M.V.R.; Takats, J. X-Ray Crystal and Molecular Structure of Tris[Hydridotris(Pyrazol-1-Yl)Borato]Ytterbium(III), Yb(HBPz3)3. *Inorg. Chem.* **1982**, *21*, 4050–4053. [[CrossRef](#)]
36. Apostolidis, C.; Rebizant, J.; Kanellakopoulos, B.; von Ammon, R.; Dornberger, E.; Müller, J.; Powietzka, B.; Nuber, B. Homoscorpionates (Hydridotris(1-Pyrazolyl)Borato Complexes) of the Trivalent 4f ions. The Crystal and Molecular Structure of [(HB(N₂C₃H₃)₃)₃Ln^{III}], (Ln = Pr, Nd). *Polyhedron* **1997**, *16*, 1057–1068. [[CrossRef](#)]
37. Apostolidis, C.; Rebizant, J.; Walter, O.; Kanellakopoulos, B.; Reddmann, H.; Amberger, H.-D. Zur Elektronenstruktur Hochsymmetrischer Verbindungen Der F-Elemente. 35 [1] Kristall- Und Molekülstrukturen von Tris(Hydrotris(1-Pyrazolyl)Borato)-Lanthanid(III) (LnTp₃; Ln = La, Eu) Sowie Elektronenstruktur von EuTp₃. *Z. Für Anorg. Und Allg. Chemie* **2002**, *628*, 2013–2025. [[CrossRef](#)]
38. Apostolidis, C.; Kovács, A.; Morgenstern, A.; Rebizant, J.; Walter, O. Tris-(Hydridotris(1-Pyrazolyl)Borato)lanthanide Complexes: Synthesis, Spectroscopy, Crystal Structure and Bonding Properties. *Inorganics* **2021**, *9*, 44. [[CrossRef](#)]
39. Reger, D.L.; Knox, S.J.; Lindeman, J.A.; Lebioda, L. Poly(Pyrazolyl) Borate Complexes of Terbium, Samarium, and Erbium. X-Ray Crystal Structure of [(.Eta.3-HB(Pz)3]2Sm(.Mu.-O2CPh)2 (Pz = Pyrazolyl Ring). *Inorg. Chem.* **1990**, *29*, 416–419. [[CrossRef](#)]
40. Chowdhury, T.; Evans, M.J.; Coles, M.P.; Bailey, A.G.; Peveler, W.J.; Wilson, C.; Farnaby, J.H. Reduction Chemistry Yields Stable and Soluble Divalent Lanthanide Tris(Pyrazolyl)Borate Complexes. *Chem. Commun.* **2023**, *59*, 2134–2137. [[CrossRef](#)]
41. Qi, H.; Zhao, Z.; Zhan, G.; Sun, B.; Yan, W.; Wang, C.; Wang, L.; Liu, Z.; Bian, Z.; Huang, C. Air Stable and Efficient Rare Earth Eu(II) Hydro-Tris(Pyrazolyl)Borate Complexes with Tunable Emission Colors. *Inorg. Chem. Front.* **2020**, *7*, 4593–4599. [[CrossRef](#)]
42. Long, J.; Lyubov, D.M.; Mahrova, T.V.; Cherkasov, A.V.; Fukin, G.K.; Guari, Y.; Larionova, J.; Trifonov, A.A. Synthesis, Structure and Magnetic Properties of Tris(Pyrazolyl)Methane Lanthanide Complexes: Effect of the Anion on the Slow Relaxation of Magnetization. *Dalt. Trans.* **2018**, *47*, 5153–5156. [[CrossRef](#)]
43. Chowdhury, T.; Horsewill, S.J.; Wilson, C.; Farnaby, J.H. Heteroleptic Lanthanide(III) Complexes: Synthetic Utility and Versatility of the Unsubstituted Bis-Scorpionate Ligand Framework. *Aust. J. Chem.* **2022**, *75*, 660–675. [[CrossRef](#)]
44. Llunell, M.; Casanova, D.; Cirera, J.; Alemany, P.; Alvarez, S. *SHAPE, Version 2.1, Program for the Stereochemical Analysis of Molecular Fragments by Means of Continuous Shape Measures and Associated Tools*; Universitat de Barcelona: Barcelona, Spain, 2013; Volume 2103.
45. Rousset, E.; Piccardo, M.; Gable, R.W.; Massi, M.; Sorace, L.; Soncini, A.; Boskovic, C. Elucidation of LMCT Excited States for Lanthanoid Complexes: A Theoretical and Solid-State Experimental Framework. *Inorg. Chem.* **2022**, *61*, 14004–14018. [[CrossRef](#)] [[PubMed](#)]
46. Görlner-Walrand, C.; Binnemans, K. Chapter 155 Rationalization of Crystal-Field Parametrization. In *Handbook on the Physics and Chemistry of Rare Earths*; Elsevier: Amsterdam, The Netherlands, 1996; pp. 121–283.
47. Arauzo, A.; Lazarescu, A.; Shova, S.; Bartolomé, E.; Cases, R.; Luzón, J.; Bartolomé, J.; Turta, C. Structural and Magnetic Properties of Some Lanthanide (Ln = Eu^{III}, Gd^{III} and Nd^{III}) Cyanoacetate Polymers: Field-Induced Slow Magnetic Relaxation in the Gd and Nd Substitutions. *Dalt. Trans.* **2014**, *43*, 12342–12356. [[CrossRef](#)] [[PubMed](#)]
48. Wu, M.-F.; Wang, M.-S.; Guo, S.-P.; Zheng, F.-K.; Chen, H.-F.; Jiang, X.-M.; Liu, G.-N.; Guo, G.-C.; Huang, J.-S. Photoluminescent and Magnetic Properties of a Series of Lanthanide Coordination Polymers with 1 H -Tetrazolate-5-Formic Acid. *Cryst. Growth Des.* **2011**, *11*, 372–381. [[CrossRef](#)]
49. Li, Y.; Zheng, F.-K.; Liu, X.; Zou, W.-Q.; Guo, G.-C.; Lu, C.-Z.; Huang, J.-S. Crystal Structures and Magnetic and Luminescent Properties of a Series of Homodinuclear Lanthanide Complexes with 4-Cyanobenzoic Ligand. *Inorg. Chem.* **2006**, *45*, 6308–6316. [[CrossRef](#)] [[PubMed](#)]
50. Xu, N.; Wang, C.; Shi, W.; Yan, S.-P.; Cheng, P.; Liao, D.-Z. Magnetic and Luminescent Properties of Sm, Eu, Tb, and Dy Coordination Polymers with 2-Hydroxynicotinic Acid. *Eur. J. Inorg. Chem.* **2011**, *2011*, 2387–2393. [[CrossRef](#)]
51. Han, M.; Li, S.; Ma, L.; Yao, B.; Feng, S.-S.; Zhu, M. Luminescent and Magnetic Bifunctional Coordination Complex Based on a Chiral Tartaric Acid Derivative and Europium. *Acta Crystallogr. Sect. C Struct. Chem.* **2019**, *75*, 1220–1227. [[CrossRef](#)]
52. De Oliveira Maciel, J.W.; Lemes, M.A.; Valdo, A.K.; Rabelo, R.; Martins, F.T.; Queiroz Maia, L.J.; de Santana, R.C.; Lloret, F.; Julve, M.; Cangussu, D. Europium(III), Terbium(III), and Gadolinium(III) Oxamate-Based Coordination Polymers: Visible Luminescence and Slow Magnetic Relaxation. *Inorg. Chem.* **2021**, *60*, 6176–6190. [[CrossRef](#)]
53. Vaz, R.C.A.; Esteves, I.O.; Oliveira, W.X.C.; Honorato, J.; Martins, F.T.; Marques, L.F.; dos Santos, G.L.; Freire, R.O.; Jesus, L.T.; Pedroso, E.F.; et al. Mononuclear Lanthanide(III)-Oxamate Complexes as New Photoluminescent Field-Induced Single-Molecule Magnets: Solid-State Photophysical and Magnetic Properties. *Dalt. Trans.* **2020**, *49*, 16106–16124. [[CrossRef](#)]
54. Shintoyo, S.; Fujinami, T.; Matsumoto, N.; Tsuchimoto, M.; Weselski, M.; Bierko, A.; Mrozinski, J. Synthesis, Crystal Structure, Luminescent and Magnetic Properties of Europium(III) and Terbium(III) Complexes with a Bidentate Benzoate and a Tripod N₇ Ligand Containing Three Imidazole, [Ln^{III}(H₃L)Benzoate](ClO₄)₂·H₂O·2MeOH (Ln^{III}=Eu^{III} and Tb^{III}). *Polyhedron* **2015**, *91*, 28–34. [[CrossRef](#)]
55. Benelli, C.; Caneschi, A.; Gatteschi, D.; Pardi, L.; Rey, P. Structure and Magnetic Properties of Linear-Chain Complexes of Rare-Earth Ions (Gadolinium, Europium) with Nitronyl Nitroxides. *Inorg. Chem.* **1989**, *28*, 275–280. [[CrossRef](#)]
56. Liu, R.; Zhao, S.; Xiong, C.; Xu, J.; Li, Q.; Fang, D. Three New One-Dimensional Lanthanide Complexes Bridged by Nitronyl Nitroxide Radicals: Crystal Structures and Magnetic Characterization. *J. Mol. Struct.* **2013**, *1036*, 107–110. [[CrossRef](#)]

57. Mei, X.; Wang, X.; Wang, J.; Ma, Y.; Li, L.; Liao, D. Dinuclear Lanthanide Complexes Bridged by Nitronyl Nitroxide Radical Ligands with 2-Phenolate Groups: Structure and Magnetic Properties. *New J. Chem.* **2013**, *37*, 3620–3626. [[CrossRef](#)]
58. Zhu, M.; Jia, L.; Li, Y.; Li, Y.; Zhang, L.; Zhang, W.; Lü, Y. Nitronyl Nitroxide Bridged 3d–4f Hetero-Tri-Spin Chains: Synthesis Strategy, Crystal Structure and Magnetic Properties. *CrystEngComm* **2018**, *20*, 420–431. [[CrossRef](#)]
59. Bain, G.A.; Berry, J.F. Diamagnetic Corrections and Pascal's Constants. *J. Chem. Educ.* **2008**, *85*, 532. [[CrossRef](#)]
60. *Apex3 Software Suite: Apex3, SADABS-2016/2 and SAINT 8.40a*; Bruker AXS Inc.: Fitchburg, WI, USA, 2017.
61. Sheldrick, G.M. SHELXT–Integrated Space-Group and Crystal-Structure Determination. *Acta Crystallogr. Sect. A Found. Adv.* **2015**, *71*, 3–8. [[CrossRef](#)]
62. Sheldrick, G.M. Crystal Structure Refinement with SHELXL. *Acta Crystallogr. Sect. C Struct. Chem.* **2015**, *71*, 3–8. [[CrossRef](#)]
63. Dolomanov, O.V.; Bourhis, L.J.; Gildea, R.J.; Howard, J.A.K.; Puschmann, H. OLEX2: A Complete Structure Solution, Refinement and Analysis Program. *J. Appl. Crystallogr.* **2009**, *42*, 339–341. [[CrossRef](#)]
64. Vostrikova, K.E. The Tripodal Ligand's 4f Complexes: Use in Molecular Magnetism. *Inorganics* **2023**, *11*, 307. [[CrossRef](#)]

Disclaimer/Publisher's Note: The statements, opinions and data contained in all publications are solely those of the individual author(s) and contributor(s) and not of MDPI and/or the editor(s). MDPI and/or the editor(s) disclaim responsibility for any injury to people or property resulting from any ideas, methods, instructions or products referred to in the content.